Applications of Polymer, Composite, and Coating Materials

Surface Functionalization and Patterning by Multifunctional Resorcinarenes

Farid Behboodi-Sadabad, Vanessa Trouillet, Alexander Welle, Phillip B. Messersmith, and Pavel A. Levkin

ACS Appl. Mater. Interfaces, **Just Accepted Manuscript** • DOI: 10.1021/acsami.8b14771 • Publication Date (Web): 18 Oct 2018

Surface Functionalization and Patterning by Multifunctional Resorcinarenes

F. Behboodi-Sadabad,[†,‡] V. Trouillet,[§,⊥] A. Welle,[⊥,∥] Phillip B. Messersmith,[#] Pavel A. Levkin[†,‡]*

[†]Institute of Organic Chemistry (IOC), Karlsruhe Institute of Technology (KIT), 76131 Karlsruhe, Germany

[‡]Institute of Toxicology and Genetics (ITG), Karlsruhe Institute of Technology (KIT), 76344 Eggenstein-Leopoldshafen, Germany

[§]Institute for Applied Materials (IAM), Karlsruhe Institute of Technology (KIT), 76344 Eggenstein-Leopoldshafen, Germany

[⊥]Karlsruhe Nano Micro Facility (KNMF), Karlsruhe Institute of Technology (KIT), 76344 Eggenstein-Leopoldshafen, Germany

[∥]Institute of Functional Interfaces (IFG), Karlsruhe Institute of Technology (KIT), 76344 Eggenstein-Leopoldshafen, Germany

[#]Departments of Materials Science and Engineering and Bioengineering, University of California Berkeley, 94720 Berkeley, USA

KEYWORDS: surface functionalization, resorcinarene, phenolic compounds, thiol-ene photochemistry, wettability

ABSTRACT: Plant phenolic compounds and catecholamines have been widely used to obtain substrate-independent precursor nanocoatings and adhesives. Nevertheless, there are downsides in using such phenolic compounds for surface modification such as formation of non-uniform coatings, need for multistep modification, and restricted possibilities for post-functionalization. In this study, inspired by strong binding ability of natural polyphenols found in plants, we used three different macrocyclic polyphenols, known as resorcin[4]arenes, to modify the surface of a different substrates by simple dip coating into the dilute solution of these compounds. Eight hydroxyl groups on the large rim of these resorcin[4]arenes provide multiple anchoring points to the surface, while the lower rim decorated with different appending groups introduces desired chemical and physical functionalities to the substrate´s surface. Deposition of a uniform and transparent resorcinarene layer on the surface was confirmed by several surface characterization techniques. Incubation of the modified substrates in different environments indicated that the stability of the resorcinarene layer was dependent on the type of substrate and the pH value. The most stable resorcinarene layer was formed on amine-functionalized substrates. The surface was modified with alkenyl functional groups in one step using a resorcinarene compound possessing four alkenyl appending groups on its small rim. Thiol-ene photoclick chemistry was used to site-selectively post-functionalize the surface with hydrophilic and hydrophobic micropatterns that was confirmed by X-ray photoelectron spectroscopy (XPS) and time-of-flight secondary ion mass spectrometry (ToF-SIMS). Thus, we demonstrate that resorcin[4]arenes extend the scope of applications of plant polyphenol and mussel-inspired precursors to tailor-made multifunctional nanocoatings, suitable for a variety of potential applications in biotechnology, biology, and material science.

1. Introduction

Inspired by the strong solid-liquid interfacial activity of plant polyphenols, various nanocoatings and adhesive precursors have been derived from plant phenolic compounds[1–5]. Similarly, adhesive coatings based on catecholamines such as dopamine (DA)[6–9] have been developed inspired by the key role of marine adhesive polyphenols present in mussel foot proteins.

A substrate-independent coating can be formed on the surface by simple immersion of a substrate into a slightly basic solution of DA or polyphenols. The presence of multiple anchoring points to the surface plays an important role for the strong interaction of polyphenols with the surface via hydrogen bonds, coordination bonds, π-π stacking or hydrophobic interactions.[10,11] Such nanocoatings have been used for surface modification and development of novel materials for biology,[12,13] material science,[14] energy research,[15,16] and various bio-medical applications[17,18]

However, there are still challenges in the usage of the coatings derived from catecholamines and plant polyphenols that limit applications of such coatings. For instance, several research groups[19–22] including ours,[2] tried to reduce nanoparticle-like structure formation in the coatings made from DA or polyphenols. Such aggregates cause high surface roughness, inhomogeneity, and subsequent weakness and instability of the coating.[19,21–23] Multistep post-functionalization[19,24] is required in order to introduce desired functional groups onto the DA and polyphenolic nanocoating precursors.[25,26] Examples include post-modification of polydopamine (PDA) layer with hydrophobic molecules or lipid-like molecules such as organic alkanethiols and alkane-phosphates.[27] Moreover, common choices for secondary functionalization are mainly limited to complexation with metal ions, boronate ester complexation, self-coupling reactions, and reaction with nucleophiles (including amine, imidazole, and thiol groups).[28–30]

Calixarenes represent building blocks for a complementary strategy for surface functionalization. Calixarenes and their derivatives have been used for sensor development,[31] cancer chemotherapy,[32] chemical separations,[33] molecular recognition,[34,35] transfection of DNA into cells,[36] and other biological applications.[37] The all-*cis* configuration on a cyclic tetramer with crown (cone) conformation in calix[4]arenes, which is the thermodynamically most stable isomer,[38–40] provides a three-dimensional structure which can be decorated with desired functional groups on the small or large rim.[39,41]

In a classical way, surface-reactive head groups on the small rim of the calixarenes were used to covalently bind calixarenes onto the surface.[42] Mattiuzzi et al.[43–45] used rigid tetrapodant calix[4]arenes as building blocks to form a monolayer on the surface by electrografting of calix[4]arene diazonium salts on the surface from their large rim side. Multivalency of calixarenes could increase their binding strengths. Using this strategy, a dense and closely packed monolayer of calix[4]arenes was formed on the surface due to the unique macrocyclic structure of the calixarene skeleton which prevents the formation of disorganized multilayers.[43]

Resorcinarenes are resorcinol-derived calixarenes.[39] Resorcin[4]arenes can easily be obtained by the acid catalyzed condensation of resorcinol with various aliphatic or aromatic aldehydes, which occurs on refluxing the reactants in a mixture of ethanol and concentrated hydrochloric acid (HCl) for several hours.[39] Usually, the cyclotetramer crystallizes from the reaction mixture in reasonable to high yields in a simple one-step untemplated reaction, although for different aldehydes different optimal reaction conditions exist.[39] In the context of surface modification, thiol-gold,[46] ion-metal coordination,[47] amine-graphene oxide,[48] silane coupling,[49] and platinum catalyzed[38] binding chemistries have been used to make a layer of resorcinarenes on surfaces.

In this paper we present a one-step strategy for surface functionalization by deploying bifunctional resorcinarenes that can adhere to different substrates including polyethylene (PE), polymethyl methacrylate (PMMA), stainless steel (steel), aluminum (Al), zinc (Zn), amine-functionalized porous poly(2-hydroxyethyl methacrylate)-co-(ethylene dimethacrylate) (poly(HEMA)),), amine-functionalized glass, and silicon wafer using their large rim side, while their small rim side can be used for the post-functionalization. The produced nanocoatings demonstrated homogeneity and transparency.

We used three different resorcin[4]arenes, compounds **1**, **2**, and **3** (**Figure 1**), as building blocks for the functionalization of different substrates. The large rim of resorcinarenes **1**, **2**, and **3** consists of eight hydroxyl groups, serving as multiple anchoring points to the surface, whereas the small rim is decorated with four methyl, undecyl, or dec-9-enyl legs, respectively. Formation of uniform, aggregate-free, and transparent nanocoatings using all three compounds **1**, **2**, and **3** was demonstrated by apparent water contact angle (WCA) measurement, UV-vis spectroscopy, XPS, and AFM analysis. By varying the choice of "legs" on the small rim, desired functional groups can be directly introduced to the surface. For instance, compound **3** was synthesized with four pendant alkenyl groups at the small rim. UV-induced thiol-ene click chemistry was used to site-selectively post-functionalize the **3**-modified surface with hydrophilic and hydrophobic functional groups, in order to tune the surface wettability against liquids possessing both high and low surface tension. This strategy could expand the choice of multifunctional building blocks for this class of bioinspired nanocoatings from catecholamines and plant phenolic compounds to tailor-made resorcinarenes.

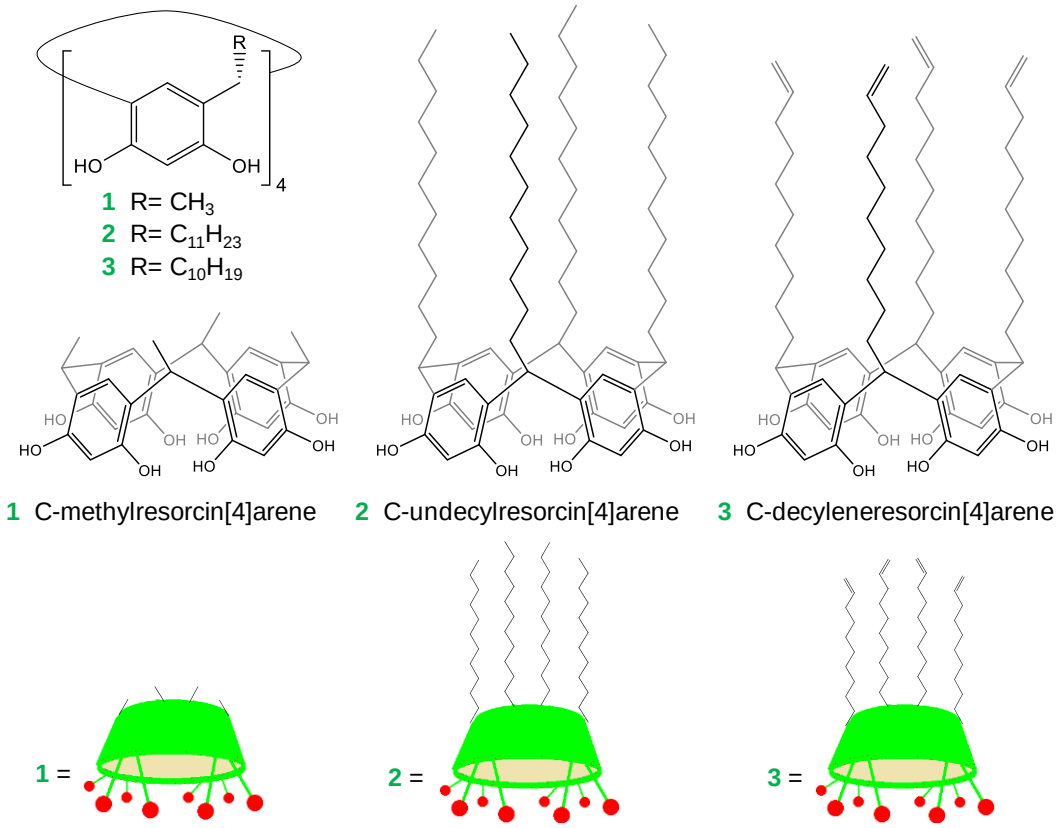

Figure 1. Chemical structures of *C*-methylresorcin[4]arene (**1**), *C*-undecylresorcin[4]arene (**2**), and designed *C*-dec-9-enylresorcin[4]arene (**3**) and their schematic representation.

2. Results and Discussion

We investigated the coating potential of resorcin[4]arenes using two commercially available resorcin[4]arenes, *C*-methylresorcin[4]arene (**1**) and *C*-undecylresorcin[4]arene (**2**). In addition, *C*-dec-9-enylresorcin[4]arene (**3**) containing four appending alkenyl groups on its small rim was synthesized according to our previous report (Figure S1,S2).[38]

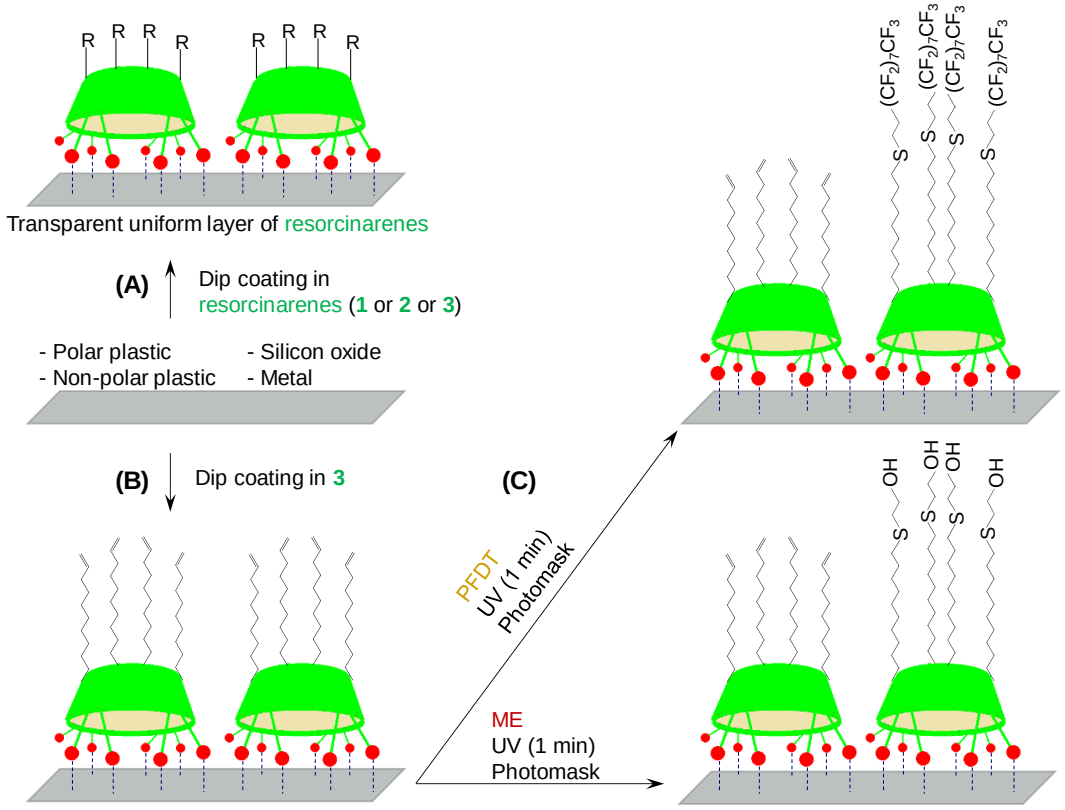

Scheme 1. (A) Formation of a uniform and transparent layer of multifunctional resorcin[4]arenes on the surface of a different of substrates by a one-step dip coating technique. (B) Modification of the surface with **3** and subsequent post-functionalization with hydrophilic (2-mercaptoethanol, ME) or hydrophobic (1*H*,1*H*,2*H*,2*H*-perfluorodecanethiol, PFDT) groups via UV-induced thiol-ene click chemistry.

To investigate coating formation ability of resorcinarenes, different substrates were immersed in a 0.8 mg/mL solution of **1**, **2**, or **3** in an ethanol:tris buffer (10 mM, pH 8.5) mixture, for 24 h at room temperature with gentle agitation (**Scheme 1**A,B). Deposition of a resorcinarene layers on the surface of different substrates including polyethylene (PE), polymethyl methacrylate (PMMA), stainless steel (steel), aluminum (Al), zinc (Zn), amine-functionalized porous poly(2-hydroxyethyl methacrylate)-*co*-(ethylene dimethacrylate) (poly(HEMA)), and silicon wafer was investigated by apparent water contact angle (WCA) measurements (**Figure 2**), XPS, and AFM analysis (**Figure 3**, Figure S3, S4). The term poly(HEMA) refers to amine-functionalized porous poly(HEMA) throughout the text and figures.

Apparent WCA and contact angle hysteresis (CAH) on flat PE, PMMA, steel, Al, Zn, and rough poly(HEMA) substrates before and after functionalization with **1**, **2** and **3** are shown in **Table 1**. All flat surfaces modified with the same compounds showed similar WCAs indicating successful functionalization and homogeneous coatings. The difference in WCAs in the case of the poly(HEMA) reflects its porous rough surface, which leads to either decrease or increase of the apparent WCA after the modification with either slightly hydrophilic **1** or hydrophobic **2** and **3**, respectively (Figure 2A,B).

Deposition kinetics of the resorcinarenes on the surface was monitored by measuring apparent water contact angle of poly(HEMA) substrate at different time intervals up to 36 h after immersing in the coating solution of **1**, **2**, and **3** (Figure 2C). Apparent contact angle reached a constant value of 16°±3, 138°±3, 137°±4 after 24 h of incubation in the coating solution of **1**, **2**, and **3**, respectively (Figure 2C).

Table 1. Apparent water contact angles (θ) and contact angle hysteresis (Δθ) of different substrates before and after modification with **1**, **2**, and **3**.

Substrate	**Bare**		**+1**		**+2**		**+3**	
	θ	Δθ	θ	Δθ	θ	Δθ	θ	Δθ
PE	86±2.1	~57	73±4.2	~60	107±4.3	~52	105±3.2	~51
PMMA	70±2.2	~46	67±4.3	~39	100±3.4	~37	103±4.6	~44
Steel	69±1.9	~33	64±3.9	~35	105±3.8	~39	102±.3.9	~34
Al	74±2.2	~42	65±3.6	~38	109±2.9	~36	107±3.8	~34
Zn	75±2.4	~54	64±4.5	~48	108±3.8	~58	106±3.5	~55
Poly(HEMA)	2±1.1	-	15±2.5	~10	138±2.6	~40	137±2.3	~43

Stability of the coated layer was investigated by monitoring apparent WCA of PE, steel, and poly(HEMA) substrates coated with **1**, **2**, and **3**, at different time intervals after immersing or sonicating the substrates into a 1:1 ethanol:water mixture for 24 h (Figure 2D for **3**, Figure S5 for compound **1**,**2**). Apparent WCA of substrates coated with **1**, **2**, and **3** remained constant after immersing in a 1:1 ethanol:water mixture over 24 h, indicating deposition of a relatively stable resorcinarene layer on the surface at the mentioned environment. Sonication of the solution led to decrease of apparent WCA of the substrates modified with **3** from 105° and 102° of the bare PE and steel substrates to 85° and 70°, respectively, indicating detachment of the resorcinarene layer from the surface within the first 6 h of sonication (Figure 2D). Detachment of the resorcinarene from the surface could be due to relatively weak and reversible non-covalent interaction of the polyphenols with the surface.[50] However, **1**, **2**, and **3** formed a much more stable layer on the amine-functionalized porous poly(HEMA), confirmed by no change in apparent WCA even after sonication for 24 h, possibly due to covalent attachment of the

phenolic groups of the resorcinarenes to the amino groups on the surface[50] via Michael addition-type reaction or Schiff base formation.[28–30]

We investigated the adhesive strength of the resorcinarene layer of **3** deposited on the steel, PE and (amine-functionalized) glass substrates by monitoring the apparent WCA of the substrates after immersing in aqueous buffer solutions at acidic (pH 3), neutral (pH 7), and basic pH (pH 9) for different time intervals (Figure S6). Apparent WCA of the substrates incubate at neutral pH didn't change after 48 h. However, apparent WCA decreased significantly after 12 h incubation in a basic (steel and PE) or in an acidic solution (amine-functionalized glass) (Figure S6). Significantly higher binding energy of bidentate hydrogen bonds in polyphenols than the binding energy of mono hydrogen bonds has been confirmed theoretically and experimentally.[51] Hydrogen bonds could be formed between the hydroxyl groups (as hydrogen donors) on resorcinarene and the oxygen atoms (as hydrogen acceptors) on the (oxidized) PE and steel substrates.[52] Generation of other types of interaction with the surface in addition to hydrogen bonds could be the reason of the stability of the resorcinarene layer on PE and steel substrates at pH 3, and pH 7 (Figure S6A,B).[52] However, in basic environment (pH 9) resorcinarene layer detached from the surface of PE and steel substrates possibility due to deprotonation of majority of the hydroxyl groups and their oxidation to quinone moieties[53] that leads to a weaker interaction with the PE and steel substrates (Figure S6A,B).

On the other hand, oxidation of hydroxyl groups to quinone moieties at basic pH, could enable covalent binding of the polyphenols to the amine-functionalized surfaces.[50] Apparent contact angle of the **3**-modified (amine-functionalized) glass substrate did not change significantly in natural (pH 7) and basic condition (pH 9), possibly due to covalent interaction with the surface (Figure S6C). However, in acidic environment (pH 3), quinone structure is favored over

hydroxyl in polyphenols.[53] Therefore, weak surface interaction between the resorcinarene layer and amine-functionalized surface observed in acidic pH (Figure S6C) could be due to the shift in the chemical equilibria of hydroxyl-quinone toward quinone structure.[50]

Dependency of the adhesion strength and the stability of the substrate-independent polyphenolic nanocoatings on the substrate type, pH of the environment, and phenolic precursor was reported in the literature.[50,52,54]

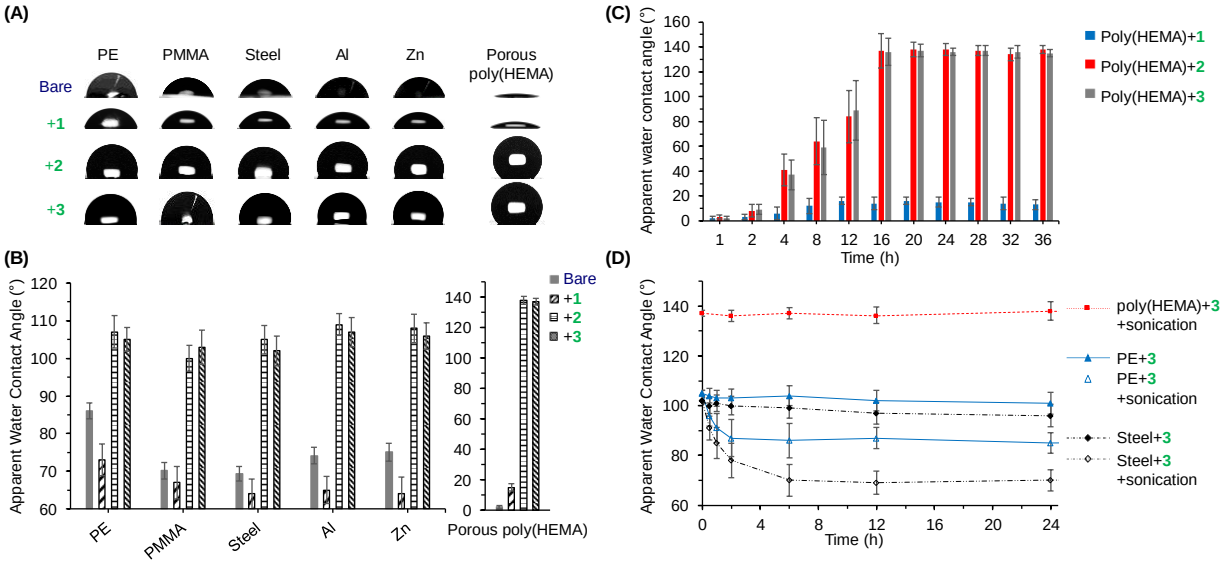

Figure 2. Deposition of resorcinarenes (**1**,**2**,**3**) on different substrates. (A) Water droplets formed on the surface of PE, PMMA, steel, Al, Zn, and amine-functionalized porous poly(HEMA) substrates before and after modification with **1**, **2**, and **3** and corresponding apparent WCA. (B) (C) Deposition kinetics of **1**, **2**, and **3** on the poly(HEMA) substrate monitored by measuring apparent water contact angle measurements after immersing the substrate in the corresponding coating solutions for different time intervals. (D) Apparent WCA of PE, steel, and poly(HEMA) substrates modified with **3** after immersion or sonication in ethanol:water 1:1 mixture for 24 h.

Deposition of a resorcinarene on the surface was investigated by XPS analysis of the substrates modified with **3**. The strong decrease of the intensity of the characteristic substrate signals proves the modification of the substrate with **3** (Figure 3A,B and Figure S3). In the case of PMMA, C 1s at 288.9 eV attributed to O=C-O group was chosen as a marker. For further metal substrates, peaks stemming from the metal itself were observed, namely Fe 2p, Al 2p, and Zn 2p doublets for steel, Al, and Zn substrates, respectively. A decrease of at least 75% of the initial intensity for the bare substrates was observed for all the mentioned peaks, which points out the presence of a new layer on the surface. Furthermore, the carbon concentration increased and more importantly the contribution of the component at 285.0 eV (C-C, C-H) in the C 1s spectra increased after surface modification. This observation supports the deposition of **3** on the surface since this compound contains long alkyl chains.

Surface topography and thickness of the resorcinarene layer deposited on a silicon wafer was analyzed using AFM. A layer free from nanoparticle-like structures was observed on the silicon surface with an average thickness of 1.0±0.15, 2.1±0.24, and 1.9±0.18 nm and mean square roughness (RMS) of 0.4, 0.6, 0.5 nm by immersion of the substrate into a coating solution of **1**, **2**, and **3**, respectively (Figure 3C,D, Figure S4). The average thickness of the resorcinarene layer was calculated by subtracting the average height of the scratched area from the average height of the unscratched area. Roughness values were similar to that of the bare substrates ($RMS_{bare\ Si}$=0.3 nm, RMS of Si substrates before modification with **1**, **2**, and **3** were 0.3 nm, 0.4 nm, 0.4 nm, respectively) indicating the deposition of a uniform layer on the whole surface. These results agree well with the theoretical height values (estimated from MM2 energy minimization using Chem3D software) of ca. 0.8, 1.9, and 1.7 nm for **1**, **2**, and **3**, respectively. AFM analysis of a smaller area (5 μm^2 squares) of the bare and modified silicon substrates with **1**, **2**, and **3**

indicated that a compact uniform layer of resorcinarenes, free from nanoparticle-like structure, formed on the surface (Figure S4). The thickness values measured by AFM were in agreement with the thickness values measured by ellipsometry, 0.9±0.12, 2.3±0.19, and 2.2±0.21 nm for the silicon substrate coated with **1**, **2**, and **3** respectively.

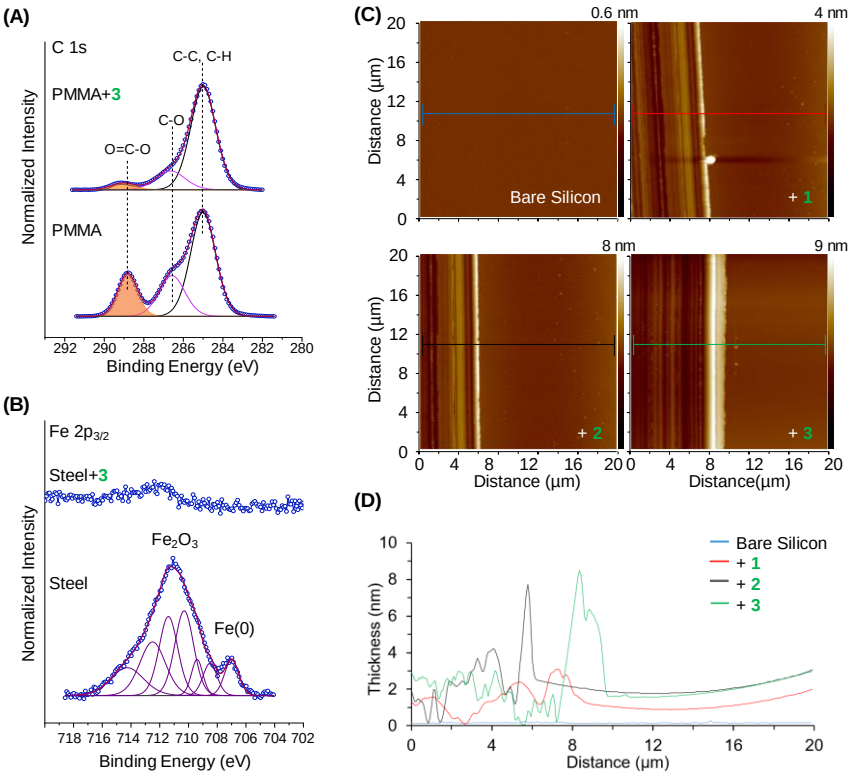

Figure 3. Surface modification using resorcinarenes (**1**,**2**,**3**). (A) Detailed C 1s and (B) Fe 2p XP spectra of PMMA and steel substrates before and after modification with **3**. (C) AFM height image of bare silicon, silicon after modification with **1**, **2**, and **3** after gentle scratching (on the left side of each sample). (D) Corresponding height profile along the lines.

In order to investigate the ability to post-functionalize the substrates modified with **3**, we used UV-induced thiol-ene click chemistry to modify dec-9-enyl pendant groups on the small rim of **3** with 2-mercaptoethanol (ME) and *1H,1H,2H,2H*-perfluorodecanethiol (PFDT) (Scheme 1C, **Figure 4**). Hydrophobic PFDT and hydrophilic ME were clicked on the **3**-modified surface by 1

min UV irradiation of PFDT and ME solutions. Apparent WCA measurements of **3**-modified poly(HEMA) and **3**-modified amine-functionalized glass substrates after post-functionalization indicated a high wettability contrast between PFDT- and ME-functionalized surface for liquids possessing both high and low surface tension (Figure 4A,B). The term glass refers to the amine-functionalized glass throughout the text and figures.

Apparent WCA of poly(HEMA) substrate increased from 2° to 137°, 152°, and 87° after modification with **3**, and post-functionalization with PFDT and ME respectively (Figure 4A). Due to the combined micro- and nanoporosity of the poly(HEMA),[55] apparent WCA reached 152° after post-functionalization with PFDT. Water droplets rolled off the PFDT-functionalized surface (tilting angle 8°), while water droplets were pinned onto the ME-functionalized surface (Movie S1). **3**-modified poly(HEMA) substrate post-functionalized with PFDT was able to repel liquids with lower surface tension such as ethylene glycol (surface tension 47.7 mN/m) and cyclohexanol (surface tension 34.4 mN/m). However, surfaces post-functionalized with ME became again completely wettable for ethylene glycol and cyclohexanol (Figure 4A).

Apparent WCA of glass substrate increased from 47° to 72°, 86°, and 61° after modification with **3**, and post-functionalization with PFDT and ME respectively (Figure 4B). **3**-modified glass after post-functionalization with PFDT was able to repel liquids with lower surface tension than water (surface tension=72.8 mN/m) including ethylene glycol (surface tension 47.7 mN/m), cyclohexanol (surface tension=34.4 mN/m), and *n*-hexane (surface tension 18.4 mN/m) (Figure 4B). By post-functionalization of the **3**-modified glass surface with ME, the contact angle of water, ethylene glycol, cyclohexanol, and *n*-hexane decreased from 72°, 55°, 19°, and 15° for the **3**-modified glass to 61°, 43°, 15°, and 6° for ME-functionalized surface. Small differences observed in the contact angles after post-functionalization with PFDT and ME (Figure 4A,B)

could be due to the chemical structure of compound **3**, which contains a large relatively hydrophobic macrocycle (of four benzene rings) with four hydrophobic long alkenyl chains. Thus, post-functionalization of **3** with hydrophilic hydroxy groups (from ME) leads to a decrease of the surface energy but not a drastic one.

Apparent WCA measurements, on one hand, confirmed post-functionalization of the substrates modified with **3** via thiol-ene click reaction, and on the other hand, demonstrated the ability to tune the surface wettability for a variety of liquids.

We investigated transparency of resorcinarene layer formed on the glass surface by measuring UV-vis spectra before and after modification of the surface with **3** and post-functionalization with PFDT and ME. UV-vis spectra indicated that glass remains transparent after deposition of the resorcinarene layer and the subsequent post-functionalization (Figure 4C).

Stability of resorcinarene layer of **3** was investigated by measuring apparent WCA at different time intervals after sonication in a 1:1 ethanol:water mixture for 24 h. Apparent WCA of **3**-modified substrates remained constant before and after post-functionalization via thiol-ene photoclick reaction further confirming deposition of a more stable resorcinarene layer on the surface (Figure 4D).

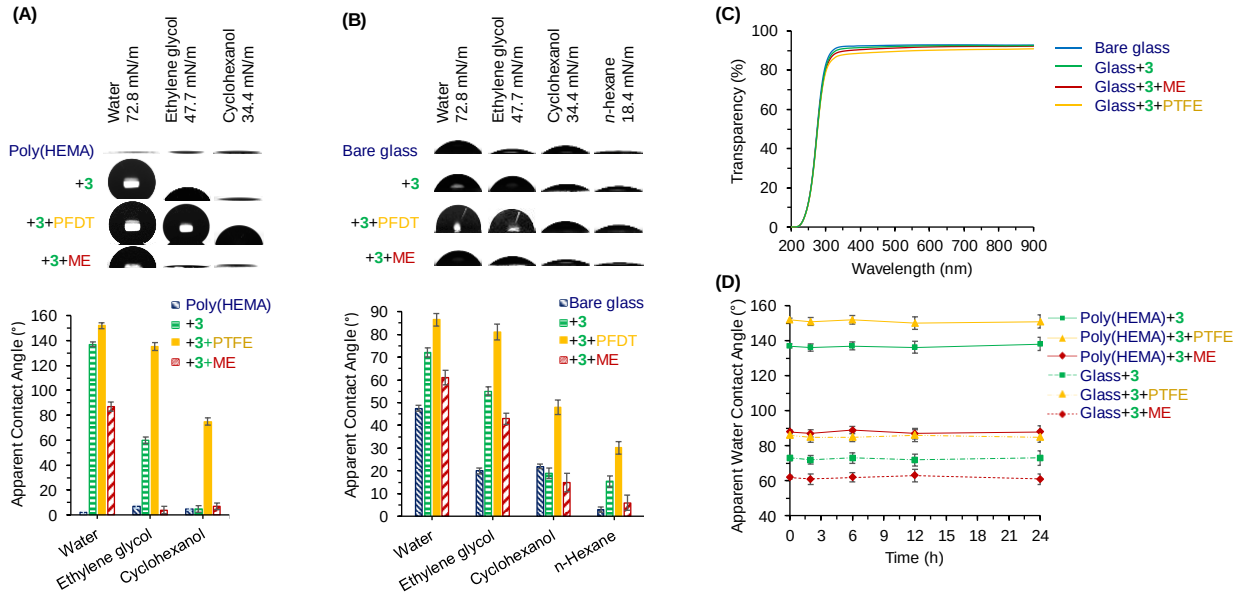

Figure 4. Tuning surface wettability by post-functionalization of **3** via UV-induced thiol-ene click chemistry. Droplets of solvents with different surface tensions formed on the surface of poly(HEMA) (A) and glass (B) after modification with **1**, **2**, and **3**, and after post-functionalization of **3**-modified surface with *1H,1H,2H,2H*-perfluorodecanethiol (PFDT) and 2-mercaptoethanol (ME) via UV-induced thiol-ene click chemistry. Corresponding apparent contact angles are shown in the graphs. (C) Transparency (%) of bare glass, **3**-modified glass, and after clicking PFDT and ME. (D) Apparent WCA of **3**-modified porous poly(HEMA) and glass substrates before and after thiol-ene reaction after sonication in ethanol:water 1:1 mixture for 24 h.

Thiol-ene photo-click chemistry is a versatile one-step procedure for spatial and temporal controlled coupling of thiol and alkene-functionalized compounds and has been used widely in materials science.[56] A layer of **3** contains alkenyl groups formed on the glass surface by immersing the substrate into the coating solution of **3** (0.8 mg/mL, in a 1:1 ethanol:tris buffer (10 mM, pH 8.5)). By UV irradiating through a photomask in the presence of PFDT and ME, we were able to control the post-functionalization of alkenyl groups spatially (**Figure 5**A). For instance, to make a micropattern of hydrophilic spots within hydrophobic borders on the **3**-

modified substrate, a solution of PFDT was filled in between the surface and a photomask followed by 1 min UV irradiation through a photomask, followed by washing and drying. Finally, a solution of ME was filled into the setup and irradiated with UV light for 1 min to introduce hydroxyl groups on the alkenyl chains of **3**, followed by washing and drying (Figure 5A).

Micropatterning of the **3**-modified surface with PFDT and ME was confirmed by XPS and ToF-SIMS (Figure 5B,C). XPS chemical mapping war first conducted in order to identify the position of the chemically different areas (Figure S7). Afterward, high energy resolution spectra could be recorded at well-defined locations evidenced by the mapping (Figure 5B). Two peaks at 291.9 eV and 294.1 eV in the C 1s spectrum and the corresponding F 1s signal at 689.0 eV proved[57] the presence of $-CF_2$ and $-CF_3$ functional groups in the PFDT-functionalized regions next to ME-functionalized regions. In another micropatterning experiment, ToF-SIMS analysis confirmed the presence of the mass fragments corresponding to F_2^- and CF_3^- in the regions modified with PFDT (Figure 5C).

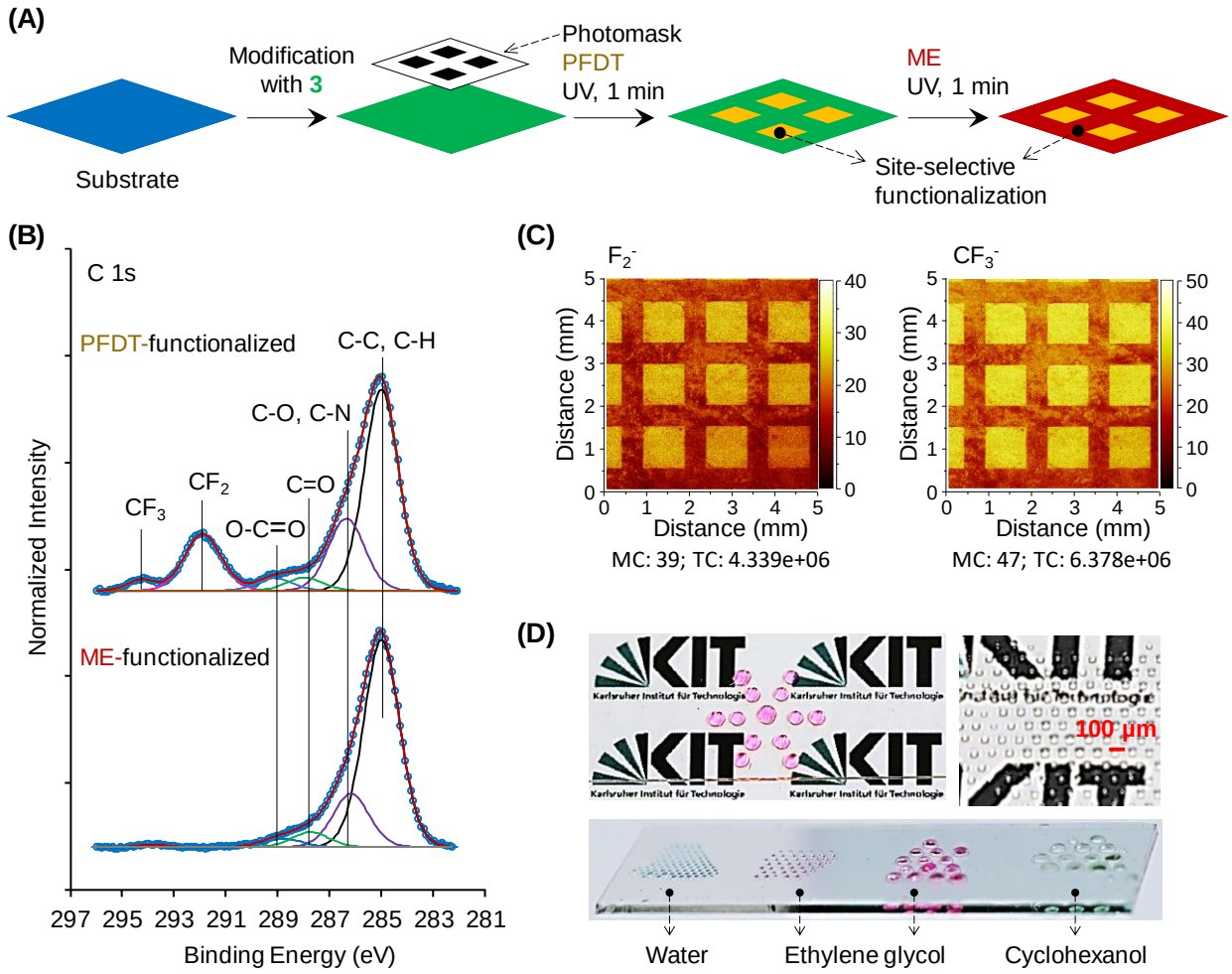

Figure 5. Photopatterning of the glass surface modified with **3** and formation of droplet microarray. (A) Schematic representation of site-selective functionalization of **3**-modified glass surface with PFDT or ME via UV-induced thiol-ene click chemistry. (B) C 1s XP spectra of the **3**-modified surface after post-functionalization with PFDT (top) and ME (bottom), indicating the formation of -CF_2 and -CF_3 functional groups on the surface after functionalization with PFDT. (C) ToF-SIMS F_2^- and CF_2^- ion intensity maps of **3**-modified surface post-functionalized with PFDT (squares) and ME (borders). (D) Droplet microarray of dyed water, ethylene glycol, and cyclohexanol formed on **3**-modified glass slide after the micropatterning.

In order to investigate the dynamic wetting behavior of the surface, advancing and receding contact angles of water, ethylene glycol, and cyclohexanol on glass substrate were measured

before and after modification with **3**, and post-functionalization with PFDT and ME (**Figure 6**). The results of static and dynamic contact angle measurements indicated that although static apparent contact angles did not change a lot after the post-functionalization with PFDT or ME, the contact angle hysteresis values showed much larger difference confirming a successful post-functionalization (Figure 6). These observations further confirmed the hypotheses that a resorcinarene layer containing bulk hydrophobic groups was deposited on all the surfaces.

Due to the high contrast of wettability between PFDT- and ME-functionalized regions (Figure 4A,B, Figure 6), droplet microarrays could be spontaneously formed on the transparent micropatterned surface by rolling a droplet of liquid, including water, ethylene glycol, or cyclohexanol on the micropatterned surface.[58]

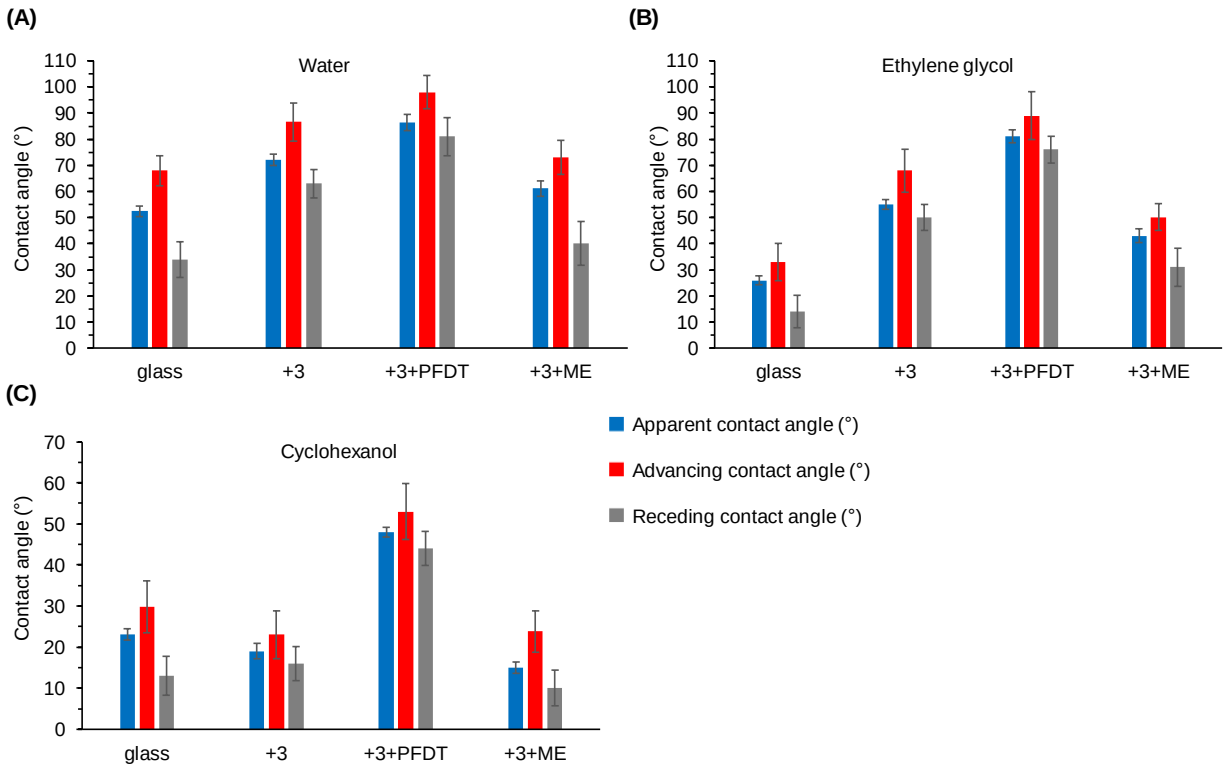

Figure 6. Apparent static, advancing, and receding contact angles of (A) water, (B) ethylene glycol, (C) cyclohexanol on (amine-functionalized) glass, before and after modification with **3**, and after post-functionalization with PTFE or ME.

3. Conclusion

Inspired by strong adhesive properties of natural polyphenols found in plant polyphenols, we developed a new strategy to use resorcinarenes as building blocks for surface functionalization. Resorcinarenes can be synthesized in a simple one-step reaction and provide eight hydroxyl groups on the large rim that serve as multiple anchor points to PE, PMMA, steel, Al, Zn, (amine-functionalized) poly(HEMA), (amine-functionalized) glass, and silicon wafer substrates, while the small rim can be decorated with desired functional groups.

We used three resorcin[4]arenes, compound **1**, **2**, and **3**, to make transparent uniform layers on the surface of plastic, metals, and silicon oxides by a single-step dip coating of the substrates in the corresponding solutions of resorcinarenes. Investigation of the stability of the resorcinarene layer on the surface indicated that the extent of stability of the resorcinarene layer on the surface was dependent on the substrate type and the pH values. Variation of the stability may be attributed to the different interaction mechanism of the polyphenols with different substrates. The most stable layer of resorcinarene was formed on amine-functionalized substrates possibly due to covalent attachment of resorcinarene to the surface.

Compound **3** decorated with alkenyl appendages on the small rim enabled post-functionalization of the surface via thiol-ene photo click chemistry. The **3**-modified glass was post-functionalized with hydrophobic or hydrophilic functional groups by UV irradiating the substrate through a photomask for 1 min in the presence of PFDT or ME. Droplet microarray of liquids with either high or low surface tension was formed on the surface of the micropatterned glass substrate by rolling a drop of the liquid over the surface.

This strategy could expand the choice of building blocks for this class of bioinspired nanocoatings from catecholamines and plant phenolic compounds to tailor-made multifunctional resorcinarenes with a wide range of potential applications in chemistry, biology, and material science.

4. Experimental Section

Materials

C-methylcalix[4]resorcinarene (**1**) and *C*-undecylcalix[4]resorcinarene monohydrate (**2**) resorcinol, 10-undecenal were purchased from Sigma-Aldrich (China, Switzerland, Germany, India, respectively). 2-Hydroxyethyl methacrylate (HEMA) and ethylene dimethacrylate (EDMA) were purchased from Sigma-Aldrich (Germany) and purified through a short column filled with basic aluminum oxide to get rid of the inhibitors. All the other chemicals were purchased from Sigma-Aldrich (Germany) and used without further purification. Formate (pH 3), phosphate (pH 7), and carbonate-bicarbonate (pH 9) buffers were prepared at 100 mM concentration.

Nexterion B glass slides were obtained from Schott AG (Mainz, Germany) and silicon wafers (CZ-Si-wafer 4 inch) from MicroChem GmbH (Berlin, Germany) were used. Polyethylene (PE), polymethyl methacrylate (PMMA), stainless steel (steel), aluminum (Al), zinc copper alloy (Zn) substrates were kindly provided by Institute of Toxicology and Genetics (ITG) at the KIT. Bare glass slides and silicon wafer substrates were cleaned by sonication for 10 min in, deionized (DI) water, 2-propanol, and acetone and dried with nitrogen gas. DI water, 2-propanol, and ethanol were used to clean other substrates by 10 min sonication followed by drying with nitrogen gas. High-purity DI water with a resistivity of 18.2 MΩ cm was obtained from an inline Millipore water purification system. Acetone and the other solvents were obtained from Merck KGaA (Germany). Tris buffers were made at 10 mM concentration at pH 8.5. The final pH value adjusted by using a Mettler Toledo digital pH meter (China).

Characterization

Mass spectrometry was performed using an ESI-MS (Bruker ESI-TOF, Institute of Nanotechnology (INT), KIT) in positive mode. ^{1}H NMR spectra were recorded on a DRX-500 (500 MHz) (Bruker, Germany), and chemical shifts were reported in ppm using residual solvent peaks as internal standards. The UV−vis absorbance (200−900 nm) of the bare and coated glass slides was measured using a Lambda 35 UV−vis spectrometer (PerkinElmer, Germany). Apparent contact angle of different liquids (~4 μL) on bare and modified substrates was measured using a Drop Shape Analyzer model DSA25S (Krüss, Hamburg, Germany). Advancing contact angles were obtained by measuring the contact angle while the liquid was slowly added (at a rate of 0.1 μL/s) from a ~4 μL droplet to 12 μL in contact with the sample and a micrometer syringe. Receding contact angles were obtained with liquid slowly retracting (at a rate of 0.1 μL/s) from a ~12 μL droplet to 4 μL. Atomic force microscopy (AFM) was performed on a Dimension Icon AFM (Bruker, Karlsruhe, Germany) in standard tapping mode in air (INT, KIT). Cantilevers used were of type HQ:NSC15/AI BS (MikroMasch) with a nominal force constant of 40 N m^{-1} and a resonance frequency of 325 kHz. The thickness of the resorcinarene layer on silicon substrates was measured using spectroscopic ellipsometry in dry state (M44, Woollam Co., Inc., Lincoln NE, USA). The ellipsometry measurements were performed at an angle of incidence of 75° in the spectral region of 370–900 nm. Ellipsometric parameters were fitted using a Cauchy model. ToF-SIMS experiments were performed on a TOF-SIMS 5 machine (ION-TOF GmbH, Münster, Germany) at the Institute of Functional Interfaces, KIT. XPS measurements were performed using a K-Alpha+ XPS spectrometer (ThermoFisher Scientific, East Grinstead, UK), IAM, KIT. Data acquisition and processing using the Thermo Advantage software is described elsewhere.[59] All coatings were analyzed using a micro-focused, monochromated Al Kα X-ray source (400 μm spot size). The K-Alpha+ charge

compensation system was employed during analysis, using electrons of 8 eV energy, and low-energy argon ions to prevent any localized charge build-up. The spectra were fitted with one or more Voigt profiles (BE uncertainty: ±0.2eV) and Scofield sensitivity factors were applied for quantification.[60] All spectra were referenced to the C 1s peak (C-C, C-H) at 285.0 eV binding energy controlled by means of the well-known photoelectron peaks of metallic Cu, Ag, and Au, respectively. The K-alpha+ snapmap option was used to image an area of 3×3 mm with an X-ray spot of 50 μm. (8 iterations were run in order to reach a better statistic).

Methods

Synthesis of *C*-dec-9-enylresorcin[4]arene (3): Compound **3** was synthesized by the acid catalyzed condensation of resorcinol with 10-undecenal by heating the reactants to reflux in a mixture of ethanol at 60°C for 16 hours according to our previous report.[38] Briefly, 12 N hydrochloric acid (32 mL was added to a solution of 10-undecenal (33.6 g, 0.2 mol) and resorcinol (22.0 g, 0.2 mol) in ethanol (200 mL) over 10 min at 0°C. The red oil that formed after stirring the mixture for 16 h at 60°C was poured into well-stirred deionized water (600 mL). The orange precipitate was filtered off and washed thoroughly with hot deionized water followed by drying. The solid product was dissolved in acetonitrile (ACN) at 40°C and kept at room temperature for 3 h. By decanting the solution, the precipitated dark oil was removed. The yellow resulting solution was concentrated around by one-third and cooled to 0°C. The solvent was decanted after precipitation of another part of the dark oil. This procedure was repeated until no more dark precipitation was formed. The solvent was removed under reduced pressure to afford about 10 g (22%) of **3**. Nuclear magnetic resonance (NMR) and mass spectrometry (ESI-MS) analysis were used to characterize compound **3**. ^{1}H NMR (500 MHz, $CDCl_3$) of **3** is shown

in Figure S1. ESI-MS (positive mode, *m/z*): $[M+Na]^+_{theor.}$=1063.6991, $[M+Na]^+_{exp.}$=1063.7035 (Figure S2).

Deposition of the resorcinarene layer on the surface: Cleaned substrates were immersed in a 0.8 mg/mL solution of **1**, **2**, or **3** in a 1:1, 3:1, or 1:1 ethanol:tris buffer (10 mM, pH 8.5) mixture, respectively, for 24 h at room temperature with a gentle agitation. Resorcinarene modified samples were then rinsed thoroughly with DI water and ethanol and dried with nitrogen gas.

Preparation of amine-functionalized surfaces: Cleaned glass-plates were immersed in 1 M NaOH for 1 h and afterward washed with deionized water followed by immersing them in 1 M HCl for 30 min, washing with deionized water and drying with a nitrogen gun. Bare glass plates were immersed into 50 mL of ethanol containing 20 %vol. (3-aminopropyl)triethoxysilane. Then, the solution was stirred at RT for 5 min. The substrates were washed with ethanol and dried with nitrogen gas. Details of the preparation of amine-functionalized micro- and nanoporous poly(HEMA) could be found in our reports.[55,61]

Post-functionalization of *C*-dec-9-enylresorcin[4]arene (3) via thiol-ene photoclick chemistry: Amine-functionalized glass or amine-functionalized porous poly(HEMA) substrates were modified with **3** according to the deposition process described above. **3**-modified substrates were wetted with ethyl acetate solution of 20 vol% of *1H,1H,2H,2H*-perfluorodecanethiol (PFDT), covered by a quartz slide, and irradiated by 5.0 $mW.cm^{-2}$ 260 nm UV light for 1 min. After removing the quartz slide, the glass was washed with ethanol and dried with nitrogen gas. For post-functionalization with 2-mercaptoethanol (ME), the **3**-modified substrates were wetted with ethanol-water (1:1) solution containing 10 wt% of ME, covered by a quartz slide, and irradiated by UV light for 1 min. The substrates was washed extensively with ethanol and dried.

Photopatterning on the 3-modified surface: The same procedure as used for post-functionalization was employed for photopatterning, however, instead of quartz slide a quartz chromium photomask was used to UV irradiate PFDT solution for 1 min. After removing the photomask, the substrate was washed with ethanol and dried. The resulting substrate was wetted again with ethanol-water (1:1) solution containing 10 wt% of ME, covered by a quartz slide, and irradiated by UV light for 1 min. The substrate was washed extensively with ethanol and dried. For ToF-SIMS analysis, the **3**-modified glass was first post-functionalized with ME by UV irradiating the ME solution through a photomask, followed by washing and subsequent post-functionalization with PFDT as described above. A droplet microarray formed on the micropatterned surface spontaneously by rolling a colored droplet of the liquid on the surface. Food dyes were used to give color to the liquids forming droplet microarray.

ASSOCIATED CONTENT

Supporting Information.

The following files are available free of charge.

Tuning the wettability of the 3-modified poly(HEMA) after post-functionalization with PFDT or ME (Movie)

^{1}H NMR spectra and ESI-MS spectra of compound **3**; Detailed Zn 2p scan and Al 2p scan of XPS spectra of Zinc copper alloy and aluminum substrates; Apparent water contact angle of PE, steel, and amine-functionalized porous poly(HEMA) substrates modified with **1** or **2**; Principal component analysis (PCA) of F 1s / XPS mapping of the **3**-modified surface after post-functionalization with PFDT and ME (PDF)

AUTHOR INFORMATION

Corresponding Author

*E-mail: levkin@kit.edu.

Notes

The authors declare no competing financial interest.

ACKNOWLEDGMENT

The research was supported by the Helmholtz Association's Initiative and Networking Fund (grant VH-NG-621) and the European Research Council starting grant (ERC-2013-StG337077-DropCellArray). The K-Alpha+ instrument was financially supported by the Federal Ministry of Economics and Technology on the basis of a decision by the German Bundestag. F.B.S thanks Karlsruhe House of Young Scientists (KHYS) for providing research travel grant.

ABBREVIATIONS

AFM, atomic force microscopy; XPS, X-ray photoelectron spectroscopy; ToF-SIMS, time-of-flight secondary ion mass spectrometry, WCA, water contact angle, DA, dopamine; PDA, polydopamine, ME, 2-mercaptoethanol; PFDT, *1H,1H,2H,2H*-perfluorodecanethiol; PE, polyethylene; PMMA, polymethyl methacrylate; steel, stainless steel; Al, aluminum; Zn, zinc; poly(HEMA), amine-functionalized porous poly(2-hydroxyethyl methacrylate)-*co*-(ethylene dimethacrylate).

REFERENCES

(1) Sileika, T. S.; Barrett, D. G.; Zhang, R.; Lau, K. H. A.; Messersmith, P. B. Colorless Multifunctional Coatings Inspired by Polyphenols Found in Tea, Chocolate, and Wine. *Angew. Chem., Int. Ed.* **2013**, *52*, 10766–10770.

(2) Behboodi-Sadabad, F.; Zhang, H.; Trouillet, V.; Welle, A.; Plumeré, N.; Levkin, P. A. Bioinspired Strategy for Controlled Polymerization and Photopatterning of Plant Polyphenols. *Chem. Mater.* **2018**., *30*, 1937-1946.

(3) Behboodi-Sadabad, F.; Zhang, H.; Trouillet, V.; Welle, A.; Plumeré, N.; Levkin, P. A. UV-Triggered Polymerization, Deposition, and Patterning of Plant Phenolic Compounds. *Adv. Funct. Mater.* **2017**, *27*, DOI: 10.1002/adfm.201700127.

(4) Rahim, M. A.; Björnmalm, M.; Bertleff-Zieschang, N.; Besford, Q.; Mettu, S.; Suma, T.; Faria, M.; Caruso, F. Rust-Mediated Continuous Assembly of Metal–Phenolic Networks. *Adv. Mater.* **2017**, *29*, DOI: 10.1002/adma.201606717.

(5) Ejima, H.; Richardson, J. J.; Caruso, F. Metal-Phenolic Networks as a Versatile Platform to Engineer Nanomaterials and Biointerfaces. *Nano Today* **2017**, *12*, 136–148.

(6) Lee, H.; Dellatore, S. M.; Miller, W. M.; Messersmith, P. B. Mussel-Inspired Surface Chemistry for Multifunctional Coatings. *Science* **2007**, *318*, 426-430.

(7) Du, X.; Li, L. X.; Li, J. S.; Yang, C. W.; Frenkel, N.; Welle, A.; Heissler, S.; Nefedov, A.; Grunze, M.; Levkin, P. A. UV-Triggered Dopamine Polymerization: Control of Polymerization, Surface Coating, and Photopatterning. *Adv. Mater.* **2014**, *26*, 8029-8033.

(8) Ryu, J. H.; Messersmith, P. B.; Lee, H. Polydopamine Surface Chemistry: A Decade of Discovery. *ACS Appl. Mater. Interfaces* **2018**, *10*, 7523–7540

(9) Du, X.; Li, L.; Behboodi-Sadabad, F.; Welle, A.; Li, J.; Heissler, S.; Zhang, H.; Plumere, N.; Levkin, P. A. Bio-Inspired Strategy for Controlled Dopamine Polymerization in Basic

Solutions. *Polym. Chem.* **2017**, *8*, 2145–2151.

(10) Schlaich, C.; Wei, Q.; Haag, R. Mussel-Inspired Polyglycerol Coatings with Controlled Wettability: From Superhydrophilic to Superhydrophobic Surface Coatings. *Langmuir* **2017**, *33*, 9508–9520.

(11) Yu, L. X.; Cheng, C.; Ren, Q. D.; Schlaich, C.; Noeske, P. L. M.; Li, W. Z.; Wei, Q.; Haag, R. Bioinspired Universal Monolayer Coatings by Combining Concepts from Blood Protein Adsorption and Mussel Adhesion. *ACS Appl. Mater. Interfaces* **2017**, *9*, 6624–6633.

(12) Ding, Y. H.; Floren, M.; Tan, W. Mussel-Inspired Polydopamine for Bio-Surface Functionalization. *Biosurface and Biotribology* **2016**, *2*, 121–136.

(13) Ye, Q.; Zhou, F.; Liu, W. M. Bioinspired Catecholic Chemistry for Surface Modification. *Chem. Soc. Rev.* **2011**, *40*, 4244–4258.

(14) Ejima, H.; Richardson, J. J.; Caruso, F. Metal-Phenolic Networks as a Versatile Platform to Engineer Nanomaterials and Biointerfaces. *Nano Today* **2016**, *12*, 136–148.

(15) Liu, Y. L.; Ai, K. L.; Lu, L. H. Polydopamine and Its Derivative Materials: Synthesis and Promising Applications in Energy, Environmental, and Biomedical Fields. *Chem. Rev.* **2014**, *114*, 5057–5115.

(16) Jeong, Y. K.; Park, S. H.; Choi, J. W. Mussel-Inspired Coating and Adhesion for Rechargeable Batteries: A Review. *ACS Appl. Mater. Interfaces* **2018**, *10,* 7562–7573.

(17) Kaushik, N. K.; Kaushik, N.; Pardeshi, S.; Sharma, J. G.; Lee, S. H.; Choi, E. H.

Biomedical and Clinical Importance of Mussel-Inspired Polymers and Materials. *Mar. Drugs* **2015**, *13*, 6792–6817.

(18) Ryu, J. H.; Hong, S.; Lee, H. Bio-Inspired Adhesive Catechol-Conjugated Chitosan for Biomedical Applications: A Mini Review. *Acta Biomater.* **2015**, *27*, 101–115.

(19) Zieger, M. M.; Pop-Georgievski, O.; Pereira, A. D.; Verveniotis, E.; Preuss, C. M.; Zorn, M.; Reck, B.; Goldmann, A. S.; Rodriguez-Emmenegger, C.; Barner-Kowollik, C. Ultrathin Monomolecular Films and Robust Assemblies Based on Cyclic Catechols. *Langmuir* **2017**, *33*, 670–679.

(20) Zhang, C.; Lv, Y.; Qin, W. Z.; He, A.; Xu, Z. K. Polydopamine Coatings with Nanopores for Versatile Molecular Separation. *ACS Appl. Mater. Interfaces* **2017**, *9*, 14437–14444.

(21) Hong, S.; Kim, J.; Na, Y. S.; Park, J.; Kim, S.; Singha, K.; Im, G.-I.; Han, D.-K.; Kim, W. J.; Lee, H. Poly(Norepinephrine): Ultrasmooth Material-Independent Surface Chemistry and Nanodepot for Nitric Oxide. *Angew. Chem., Int. Ed.* **2013**, *52*, 9187–9191.

(22) Cho, J. H.; Katsumata, R.; Zhou, S. X.; Kim, C. Bin; Dulaney, A. R.; Janes, D. W.; Ellison, C. J. Ultrasmooth Polydopamine Modified Surfaces for Block Copolymer Nanopatterning on Flexible Substrates. *ACS Appl. Mater. Interfaces* **2016**, *8*, 7456–7463.

(23) Zhang, C.; Ou, Y.; Lei, W. X.; Wan, L. S.; Ji, J.; Xu, Z. K. CuSO4/H2O2-Induced Rapid Deposition of Polydopamine Coatings with High Uniformity and Enhanced Stability. *Angew. Chem., Int. Ed.* **2016**, *55*, 3054–3057.

(24) Ge, H.; Kong, Y.; Pan, Y.; Deng, L.; Shou, D.; Lu, Q. Polydopamine Core Half-

Polyamidoamine Dendrimers Based Drug-Delivery Platform and Characterization by Electrochemical Impedance Spectroscopy. *J. Electrochem. Soc.* **2015**, *162*, G87–G93.

(25) Huang, S. Y.; Zhang, Y.; Shi, J. F.; Huang, W. P. Superhydrophobic Particles Derived from Nature-Inspired Polyphenol Chemistry for Liquid Marble Formation and Oil Spills Treatment. *ACS Sustainable Chem. Eng.* **2016**, *4*, 676–681.

(26) Faure, E.; Falentin-Daudre, C.; Jerome, C.; Lyskawa, J.; Fournier, D.; Woisel, P.; Detrembleur, C. Catechols as Versatile Platforms in Polymer Chemistry. *Prog. Polym. Sci.* **2013**, *38*, 236–270.

(27) You, I.; Jeon, H.; Lee, K.; Do, M.; Seo, Y. C.; Lee, H. H. A.; Lee, H. H. A. Polydopamine Coating in Organic Solvent for Material-Independent Immobilization of Water-Insoluble Molecules and Avoidance of Substrate Hydrolysis. *J. Ind. Eng. Chem.* **2017**, *46*, 379–385.

(28) Krogsgaard, M.; Nue, V.; Birkedal, H. Mussel-Inspired Materials: Self-Healing through Coordination Chemistry. *Chem. - Eur. J.* **2016**, *22*, 844–857.

(29) Barclay, T. G.; Hegab, H. M.; Clarke, S. R.; Ginic-Markovic, M. Versatile Surface Modification Using Polydopamine and Related Polycatecholamines: Chemistry, Structure, and Applications. *Adv. Mater. Interfaces* **2017**, *4*, DOI: 10.1002/admi.201601192.

(30) Yang, J.; Stuart, M. A. C.; Kamperman, M. Jack of All Trades: Versatile Catechol Crosslinking Mechanisms. *Chem. Soc. Rev.* **2014**, *43*, 8271–8298.

(31) Mokhtari, B.; Pourabdollah, K. Application of Calixarenes in Development of Sensors. *Asian J. Chem.* **2013**, *25*, 1–12.

(32) Yousaf, A.; Hamid, S. A.; Bunnori, N. M. Applications of Calixarenes in Cancer Chemotherapy. *Drug Des., Dev. Ther.* **2015**, *9*, 2831–2838.

(33) Li, N.; Harrison, R. G.; Lamb, J. D. Application of Resorcinarene Derivatives in Chemical Separations. *J. Inclusion Phenom. Macrocyclic Chem.* **2014**, *78*, 39–60

(34) Zhang, F.; Sun, Y.; Tian, D.; Shin, W. S.; Kim, J. S.; Li, H. Selective Molecular Recognition on Calixarene-Functionalized 3D Surfaces. *Chem. Commun.* **2016**, *52*, 12685–12693.

(35) Joseph, R.; Rao, C. P. Ion and Molecular Recognition by Lower Rim 1,3-Di-Conjugates of Calix[4]Arene as Receptors. *Chem. Rev.* **2011**, *111*, 4658–4702

(36) Samanta, K.; Ranade, D. S.; Upadhyay, A.; Kulkarni, P. P.; Rao, C. P. A Bimodal, Cationic, and Water-Soluble Calix[4]arene Conjugate: Design, Synthesis, Characterization, and Transfection of Red Fluorescent Protein Encoded Plasmid in Cancer Cells. *ACS Appl. Mater. Interfaces* **2017**, *9*, 5109–5117.

(37) Nimse, S. B.; Kim, T. Biological Applications of Functionalized Calixarenes. *Chem. Soc. Rev.* **2013**, *42*, 366–386.

(38) Levkin, P. A.; Ruderisch, A.; Schurig, V. Combining the Enantioselectivity of a Cyclodextrin and a Diamide Selector in a Mixed Binary Gas-Chromatographic Chiral Stationary Phase. *Chirality* **2006**, *18*, 49–63.

(39) Jain, V. K.; Kanaiya, P. H. Chemistry of Calix 4 Resorcinarenes. *Russ. Chem. Rev.* **2011**, *80*, 75–102.

(40) Böhmer, V. Calixarenes, Macrocycles with (Almost) Unlimited Possibilities. *Angew. Chem., Int. Ed.* **1995**, *34*, 713–745.

(41) Tauran, Y.; Coleman, A. W.; Perret, F.; Kim, B. Cellular and in Vivo Biological Activities of the Calix [n] Arenes. *Curr. J. Org. Chem.* **2015**, *19*, 2250–2270.

(42) Kim, H. J.; Lee, M. H.; Mutihac, L.; Vicens, J.; Kim, J. S. Host-Guest Sensing by Calixarenes on the Surfaces. *Chem. Soc. Rev.* **2012**, *41*, 1173–1190.

(43) Mattiuzzi, A.; Jabin, I.; Mangeney, C.; Roux, C.; Reinaud, O.; Santos, L.; Bergamini, J.-F.; Hapiot, P.; Lagrost, C. Electrografting of Calix[4]arenediazonium Salts to Form Versatile Robust Platforms for Spatially Controlled Surface Functionalization. *Nat. Commun.* **2012**, *3*, DOI:10.1038/ncomms2121.

(44) Santos, L.; Mattiuzzi, A.; Jabin, I.; Vandencasteele, N.; Reniers, F.; Reinaud, O.; Hapiot, P.; Lhenry, S.; Leroux, Y.; Lagrost, C. One-Pot Electrografting of Mixed Monolayers with Controlled Composition. *J. Phys. Chem. C* **2014**, *118*, 15919–15928.

(45) De Leener, G.; Evoung-Evoung, F.; Lascaux, A.; Mertens, J.; Porras-Gutierrez, A. G.; Le Poul, N.; Lagrost, C.; Over, D.; Leroux, Y. R.; Reniers, F.; Hapiot, P.; Le Mest, Y.; Jabin, I.; Reinaud, O. Immobilization of Monolayers Incorporating Cu Funnel Complexes onto Gold Electrodes. Application to the Selective Electrochemical Recognition of Primary Alkylamines in Water. *J. Am. Chem. Soc.* **2016**, *138*, 12841–12853.

(46) Balasubramanian, R.; Kwon, Y. G.; Wei, A. Encapsulation and Functionalization of Nanoparticles in Crosslinked Resorcinarene Shells. *J. Mater. Chem.* **2007**, *17*, 105–112.

(47) Xiong, D.; Li, H. Colorimetric Detection of Pesticides Based on Calixarene Modified Silver Nanoparticles in Water. *Nanotechnology* **2008**, *19*, DOI: 10.1088/0957-4484/19/46/465502.

(48) Zhou, J.; Chen, M.; Diao, G. W. Assembling Gold and Platinum Nanoparticles on Resorcinarene Modified Graphene and Their Electrochemical Applications. *J. Mater. Chem. A* **2013**, *1*, 2278–2285.

(49) Ruderisch, A.; Iwanek, W.; Pfeiffer, J.; Fischer, G.; Albert, K.; Schurig, V. Synthesis and Characterization of a Novel Resorcinarene-Based Stationary Phase Bearing Polar Headgroups for Use in Reversed-Phase High-Performance Liquid Chromatography. *J. Chromatogr. A* **2005**, *1095*, 40–49.

(50) Lee, H.; Scherer, N. F.; Messersmith, P. B. Single-Molecule Mechanics of Mussel Adhesion. *Proc. Natl. Acad. Sci. U. S. A.* **2006**, *103*, 12999–13003.

(51) Yu, J.; Kan, Y.; Rapp, M.; Danner, E.; Wei, W.; Das, S.; Miller, D. R.; Chen, Y.; Waite, J. H.; Israelachvili, J. N. Adaptive Hydrophobic and Hydrophilic Interactions of Mussel Foot Proteins with Organic Thin Films. *Proc. Natl. Acad. Sci. U. S. A.* **2013**, *110*, 15680-15685.

(52) Lu, Q. Y.; Danner, E.; Waite, J. H.; Israelachvili, J. N.; Zeng, H. B.; Hwang, D. S. Adhesion of Mussel Foot Proteins to Different Substrate Surfaces. *J. R. Soc., Interface* **2013**, *10*, DOI: 10.1098/rsif.2012.0759.

(53) Quideau, S.; Deffieux, D.; Douat-Casassus, C.; Pouysegu, L. Plant Polyphenols: Chemical Properties, Biological Activities, and Synthesis. *Angew. Chem., Int. Ed.* **2011**, *50*, 586–621.

(54) Barrett, D. G.; Sileika, T. S.; Messersmith, P. B. Molecular Diversity in Phenolic and Polyphenolic Precursors of Tannin-Inspired Nanocoatings. *Chem. Commun.* **2014**, *50*, 7265–7268.

(55) Geyer, F. L.; Ueda, E.; Liebel, U.; Grau, N.; Levkin, P. A. Superhydrophobic-Superhydrophilic Micropatterning: Towards Genome-on-a-Chip Cell Microarrays. *Angew. Chem., Int. Ed.* **2011**, *50*, 8424–8427.

(56) Xi, W. X.; Scott, T. F.; Kloxin, C. J.; Bowman, C. N. Click Chemistry in Materials Science. *Adv. Funct. Mater.* **2014**, *24*, 2572–2590.

(57) Reshetenko, T. V; St-Pierre, J.; Artyushkova, K.; Rocheleau, R.; Atanassov, P.; Bender, G.; Ulsh, M. Multianalytical Study of the PTFE Content Local Variation of the PEMFC Gas Diffusion Layer. *J. Electrochem. Soc.* **2013**, *160*, F1305–F1315.

(58) Feng, W. Q.; Li, L. X.; Du, X.; Welle, A.; Levkin, P. A. Single-Step Fabrication of High-Density Microdroplet Arrays of Low-Surface-Tension Liquids. *Adv. Mater.* **2016**, *28*, 3202–3208.

(59) Parry, K. L.; Shard, A. G.; Short, R. D.; White, R. G.; Whittle, J. D.; Wright, A. ARXPS Characterisation of Plasma Polymerised Surface Chemical Gradients. *Surf. Interface Anal.* **2006**, *38*, 1497–1504.

(60) Scofield, J. H. Hartree-Slater subshell photoionization cross-sections at 1254 and 1487 eV. *J. Electron Spectrosc. Relat. Phenom.* **1976**, *8*, 129–137.

(61) Feng, W. Q.; Li, L. X.; Ueda, E.; Li, J. S.; Heissler, S.; Welle, A.; Trapp, O.; Levkin, P. A.

Surface Patterning via Thiol-Yne Click Chemistry: An Extremely Fast and Versatile Approach to Superhydrophilic-Superhydrophobic Micropatterns. *Adv. Mater. Interfaces* **2014**, *1*. DOI: 10.1002/admi.201400269.

SYNOPSIS

Inspired by the adhesive role of natural polyphenols found in plant phenolic compounds, we developed a new strategy to use multifunctional resorcinarenes as building blocks for surface nanocoatings via a single-step dip-coating. Functionalization of the surface with a resorcinarene decorated with peripheral alkenyl groups enables facile surface post-functionalization and patterning via the UV-induced thiol-ene reaction.

KEYWORDS: surface functionalization, resorcinarene, phenolic compounds, thiol-ene photochemistry, wettability

*F. Behboodi-Sadabad, V. Trouillet, A. Welle, Phillip B. Messersmith, Pavel A. Levkin**

Surface Functionalization and Patterning by Multifunctional Resorcinarenes